Linking exploratory scenarios to process-informed insights in climate vulnerability assessments

John Kucharski, Wyatt Arnold, Scott Steinschneider, Rahat Saiful, Jennifer Olszewski, Patrick Ray, Romain Maendley, and Jon Herman

Abstract

The threat that climate change poses to water resource systems has led to a significant and growing number of impact studies. These studies tend to follow two general methodological approaches: top-down, process-based studies are driven by projections of future climate change supplied by downscaled general circulation models, while exploratory scenarios drive bottom-up, vulnerability-based studies. Top-down studies generate realistic climate scenarios, but computational burdens limit the number of evaluated scenarios. As a result, critical vulnerabilities may be left unexplored. Bottom-up approaches make it possible to assess a wide range of scenarios. Still, a lack of process-informed insight makes it difficult to evaluate the plausibility of those scenarios, limiting their utility in adaptive planning. This paper evaluates process-informed exploratory scenarios that bridge the gap between top-down and bottom-up methods. This hybrid approach yields several advantages. First, emerging vulnerabilities associated with the non-linear change are linked to thermodynamic and dynamic climate drivers modeled in the GCMs with differential likelihoods and plausible ranges of change. This provides a transparent link between vulnerability and likelihood. Second, shifts in vulnerability are communicated through changes in synthetic events with clear historical analogs. This establishes an obvious benchmark through which the impacts of climate change can be understood. Finally, this hybrid approach paves the way for future work tying dynamic adaptation plans to process-informed monitoring variables.

Introduction

The challenge of water resource planning and management under climate change has led to a growing number of impact studies. Nearly all these studies are guided by one of two general approaches, and the selection of a methodological approach is rife with tradeoffs. Top-down methods driven by general circulation model (GCM) projections produce a physically realistic but limited set of climate scenarios. As a result, often concern persists that decision-relevant vulnerabilities associated with plausible but unmodeled future conditions or compounding uncertainties in climate, hydrologic, and water resource systems models may not be unidentified (Fowler et al., 2007; R. L. Wilby & Dessai, 2010). On the other hand, bottom-up approaches represent a computationally efficient alternative that asserts the ability to test a wide range of plausible future conditions (C. Brown et al., 2012; Lempert, 2019; Mendoza et al., 2018; Ray & Brown, 2015). However, in practice, the scenario generation process is often restricted to delta shifts in temperature and mean annual precipitation (Steinschneider et al., 2019). This exposes bottom-up applications to criticism since it is often unclear if these overly simplistic scenarios represent physically plausible future conditions. This paper demonstrates a middle ground between top-down and bottom-up approaches that retains the physical consistency of top-down methods while not sacrificing bottom-up methods' ability to identify vulnerabilities through a broad range of plausible future conditions.

GCMs first emerged as mathematical models of the Earth's climate system in the mid 20th century (Phillips, 1956) and contained insight used to make early predictions of anthropogenic climate change (Revelle et al., 1965). Computational limitations restrict their outputs to coarse spatial scales, with modern GCMs producing results for 50 – 100km grid cells (Karger et al., 2020). At this scale, they are unable to resolve mesoscale process, land-sea interactions, and the impact of topography on basin-scale hydrology (Teutschbein & Seibert, 2012). Therefore, downscaling GCM outputs to produce projections of local relevant weather consistent with larger-scale processes represented in the GCMs has always been a feature of top-down hydrologic impact studies, which began to appear in the 1980's climate change literature (Grotch & MacCracken, 1991).

Previous bottom-up studies have generally not systematically linked the exploratory scenarios to climate processes represented in the GCMs. However, the tools employed in creating exploratory scenarios, like stochastic weather generators, play a prominent role in top-down, downscaling procedures (R. Wilby et al., 2004). In general, these tools represent a computationally efficient means of creating ensembles of synthetic exploratory scenarios used to test the system's sensitivity to sources of substantial uncertainty. Overall, these exploratory scenarios represent a fundamental shift in the purpose of modeling,

away from prediction-oriented surrogate modeling in favor of decision-centric vulnerability assessments (Bankes, 1993).

The lack of process-informed insight in the exploratory scenario generation process is a critical weakness of past bottom-up vulnerability assessments, in part because commonly perturbed variables like average temperature and annual precipitation represent brute force modulators that aggregate multiple climate processes. Naïve shifts in these parameters, without physical basis, can produce improbable future conditions and undercut key advantages of stochastic scenario generation tools and exploratory analyses by (1) limiting the potential of these tools to test vulnerabilities to components of climate change that more directly target system performance, and (2) represented changes with differing magnitudes and levels of agreement in the GCMs. Importantly, physical insights allow exploratory scenarios to be crafted from components of climate change that are treated like a set of independent dials that can be adjusted to sample variables or combinations of variables within plausible ranges of change. This makes it possible to design experiments that causally link non-linear system responses to individual components of climate change (Quinn et al., 2018) and proxy variables that may be monitored over time. This contrasts with process based GCMs that serve as a surrogate for the actual climate system, where multiple processes and their uncertainties are resolved endogenously in the production of a single output. This yields a realistic representation of climate change, but makes it challenging to test competing hypotheses about the system's vulnerability to specific climate drivers (Zscheischler et al., 2018).

In this paper, exploratory scenarios, created by a stochastic weather generator are linked to thermodynamic and dynamic contribution to climate change modeled in the GCMs. The climate in the GCMs is modeled through a system of equations that model or approximate thermodynamic and dynamic processes (Allan et al., 2020; Seager et al., 2010). Thermodynamic changes associated with climate change are those modeled as a direct function of increased heat. Generally, these are thought of as first-order impacts related to climate change, including increases and temperature, but also slightly more nuanced shifts. For instance, increases in the amount of water vapor in the atmosphere tied to acceleration of the water cycle and increases the intensity of extreme precipitation (Barton et al., 2016; Lenderink et al., 2017; Martinkova & Kysely, 2020). Dynamical contributions to climate change are shifts in atmospheric circulation patterns; for instance, the potential expansion of subtropical dry zones or wavier jet stream patterns linked to the occurrence of heatwaves and droughts in some locations and floods in others (Blackport & Screen, 2020; J. R. Brown et al., 2020; Cai et al., 2012; Kornhuber et al., 2019).

The generation of exploratory climate scenarios linked to thermodynamic and dynamic insight yields several benefits. First, thermodynamic and dynamic processes relate climate to extreme events of concern to water resource managers. This is true in a general sense (Schlef et al., 2019; Vigaud et al., 2018) and in the case of specific events like the 2013 to 2016 California drought (Swain, 2015; Ullrich et al., 2018) or flooding associated with Hurricane Harvey (Quinn et al., 2018; Trenberth et al., 2018). Since operational decisions in water resource systems tend to be made in direct response to historical events, synthetically generated events with historical analogs can provide a benchmark through which the impact of climate change on system performance can be better understood (Herman et al., 2016).

Second, perturbations linked to process-based insight, such as shifts in temperature and mean annual precipitation, can be more convincingly assessed for plausibility and likelihood than less process-informed climate perturbations. For instance, while the GCMs signal broad agreement regarding the likelihood, direction, and approximate magnitude of increased intensity of extreme precipitation events associated with thermodynamically driven Clausius-Clapeyron scaling, there is far less agreement about the direction and magnitude of changes in extreme precipitation associated with dynamical shifts in circulation patterns (Pfahl et al., 2017). Process-informed exploratory scenarios make it easier to leverage insights accumulated across the ensemble of GCMs. Individual GCMs display different strengths and weaknesses in their ability to accurately model the climate of a specific region or represent specific thermodynamic and dynamic processes (Wehrli et al., 2018). In top-down studies, analysts often face a difficult set of tradeoffs in selection a model or set of models with known and unknow biases. By decoupling the depiction of process-informed insight from its representation in specific GCMs, exploratory scenarios can reproduce features of GCMs without incorporating model specific biases.

Third, many water resource system vulnerabilities and climate extremes are driven by compound events associated with the occurrence of multiple hazards, or climate modulated drivers. For example, rain on snow floods occur when a basin is primed for flooding through the accumulation of snow prior to an rain event (Zscheischler et al., 2018, 2020). To better understand non-linear shifts in flood risk associated with climate change, it is helpful to be able to independently evaluate changes to the precondition (i.e., the antecedent snowpack) and the rain event before assessing the combined impact on the preconditioned rain event). It is also helpful to link these changes to interconnected physical processes, in this case thermodynamic driven warming and increases in extreme precipitation.

The paper demonstrates the utility of process-informed exploratory scenarios in climate vulnerability assessments through a case study of the Tuolumne River Watershed in California. The

objective of this investigation is to present a hybrid methodology for climate impact studies, this approach offers a middle ground between top-down and bottom-up approaches that have dominated climate impact assessments for decades. It leverages process-based insights embedded in top-down approaches while not sacrificing the computational efficiency or experimental design of bottom-up approaches. Its case study provides a physical basis for traditional bottom-up stress test scenarios, typically guided by delta shifts in temperature and annual precipitation; while also demonstrating how nuanced forms of climate change represented in GCMs can be incorporated to target water resource system flood and drought vulnerabilities directly.

Data Sources

This paper evaluates thermodynamic and dynamically guided climate scenarios generated by a process-informed stochastic weather generator. Some key features of the weather generator are described in the methods section and the overall tool is described in (Steinschneider et al., 2019). Flood and drought related risks associated with these scenarios are evaluated in the Tuolumne River Watershed in California. The data used for this study includes data used in the production of the exploratory climate scenarios and water resources system modeling in the Tuolumne River Watershed. The weather generator draws on the following data sources: (1) the atmospheric pressure at 500 hPa of geopotential height taken from the NCEP/NCAR Reanalysis data (Kalnay et al., 1996) is used to model daily weather regimes, (2) Livneh daily continental United States (CONUS) metrological and hydro-meteorological (Livneh et al., 2013) data is used to simulate daily precipitation, temperature and net downward radiation in the weather simulations, and (3) the North American Land Data Assimilation System 2 (NLDAS-2) data record (Cosgrove et al., 2003) is used to distribute the daily Livneh temperature and precipitation across the hours of each simulated day. Climate scenarios generated by the weather generator are then evaluated in the US Army Corps of Engineers (USACE) Hydrologic Engineering Center (HEC) Watershed Assessment Tool (WAT), which integrates the HEC Hydrologic Model System (HMS), Reservoir Simulation (ResSim), River Analysis (RAS) and Flood Impact Assessment (FIA) simulation models. These software models are described in more detail in the USACE HEC website" (“HEC-WAT,” 2021). The reservoir operations models for Cherry Creek, Eleanor, Hetch Hetchy and New Don Pedro Reservoirs were constructed from data contained in the New Don Pedro Federal Energy Regulatory Commission (FERC) project documents" (“Don Pedro Project Relicensing FERC No.2299 - Home,” 2021). Model calibration and validation were primarily performed with data taken from the California Data Exchange Center (CDEC) (“California Data Exchange Center,” 2021).

Methods

The case study in this paper compares the impact of 72 stochastically generated climate scenarios on flood and drought risks at New Don Pedro Dam, in the Tuolumne River Watershed. This section proceeds as follows: salient details regarding the weather and scenario generation process are reviewed, followed by a description of the Tuolumne River Watershed and water resources system. Finally, the data analysis process is described.

Weather Generator

The stochastic weather generator used in this experiment is a hierarchical, semi-parametric model capable of producing multi-site, multi-variate ensembles of daily and sub-daily gridded weather simulations. This model, including its simulation of the Tuolumne River watershed climate, is the subject of (Steinschneider et al., 2019), and an earlier, but still relevant version of the model is also described in (Steinschneider & Brown, 2013). Here, two important components of the weather generator are discussed.

The weather generator is run as a series of interconnected hierarchical modules, with the output of earlier components conditioning the results produced by modules run later in the weather generation process. As a rule, processes that are apparent at larger spatial-temporal scales are simulated before those that generate finer scale information. This allows insights from climate processes in the GCMs, which are typically represented with the most credibility at regional to global scales to be introduced as an exogenous forcings that condition the generation of catchment and sub-catchment scale weather. For instance, the weather generator models low-frequency signals in interannual precipitation through a Wavelet Autoregressive Model (WARM). In many locations around the world, including the Tuolumne River Watershed, this low-frequency variability in interannual precipitation is strongly correlated with regional to hemispheric scale sea surface temperature anomalies like the El Niño Southern Oscillation (ENSO) (McCabe & Dettinger, 1999; Redmond & Koch, 1991). The weather generator module emulating this large-scale spatiotemporal oscillation in interannual precipitation totals runs first in a weather generator simulation, allowing seasonal-to-daily level weather can be conditioned on ENSO teleconnection patterns in the data.

The weather generator models *weather regimes* as an intermediate step connecting larger-scale atmospheric processes with daily catchment scale weather. Weather regimes are seasonally recurrent regional patterns of atmospheric flow that persist for days to weeks over fixed geographic locations. These dynamical components of the climate organize all synoptic scale weather in the mid-latitudes (Robertson & Ghil, 1999). In the weather generator, they are modeled as a latent state in a Markov process. More

precisely, within the context of a simulation block of days in the instrumental record are sampled based on a match between the occurrence of a specific weather regime in the observational record and the modeled weather regime in the simulation. This approach preserves many of the multi-day space-time properties associated with storms and weather patterns more generally. It also provides an opportunity to represent dynamical sources of climate change, since the frequency and persistence of these patterns of atmospheric flow are modulated by the climate state.

Climate Scenarios

The analysis presented herein includes 72 climate scenarios, one of which is the baseline climate condition used as a control in the study. The other climate scenarios include combinations of climate perturbations that can broadly be grouped in to four categories: (1) perturbations to temperature that are used to generate climate scenarios and condition other thermodynamic perturbations; (2) "traditional" bottom-up perturbations to mean annual precipitation that are explicitly linked to levels of thermodynamic change defined by the change in temperature; (3) increases in the intensity of extreme precipitation, known as Clausius-Clapeyron scaling, linked in theory and recent observation to thermodynamically driven increases in vapor content of the atmosphere (Lenderink et al., 2017; Martinkova & Kysely, 2020); and (4) an increase in the variability of the ENSO (El Niño/La Niña) cycles, based on hypothesized shifts found in a large number of GCM based experiments (Fredriksen et al., 2020; Yun et al., 2021). This perturbation to the intensity of the ENSO signal shows up in California (and in the weather generator simulations) as a dynamic perturbation that affects the frequency and persistence of the weather regimes, which strong precondition simulated daily temperature and precipitation.

These perturbations in combination produce 72 climate scenarios that can be used tie non-linear vulnerabilities to specific climate processes: (1) 4 temperature (+0, 2, 3, 4 degrees Celsius increases), (2) 3 annual mean precipitation (-3, 0, 3 percent shifts per degree of warming), (3) 3 Clausius-Clapeyron scaling (0, 7, 14 percent shifts in the daily rainfall distribution per degree of warming), and (4) 2 ENSO variability (1, 2x the historical variability).[1] To distinguish between natural variability and climate signal, each of the 72-climate scenarios is composed of 33 weather generator traces containing 30 years of hourly data across 28 subbasin locations.

[1] Not all this data is currently available. Therefore, the results presented in this paper focus on the 4 temperature perturbations, 3 annual precipitation perturbations and 2 of the Clausius-Clapeyron perturbations. These perturbations produce a total of 4 x 3 x 2 = 24 climate scenarios.

Tuolumne River Watershed

The Tuolumne River Watershed is in the San Joaquin Valley in California's central valley. It occupies just under 5,000 square kilometers, making it approximately the same size as the state of Rhode Island. Its climatology is broadly defined by its location in California's central valley, which is subject to a semi-arid Mediterranean climate with cool wet winters, hot dry summers, and a high degree of interannual variability, as well as its steep topographic gradient. Over 148 river miles from its outlet with the San Joaquin River, it rises from near sea level (26 ft) to over 14,000 ft near the summit of Mount Lyell and the terminus of the Lyell glacier. By discharge, it is the largest river in the Southern Sierra Nevada Mountains with an estimated full natural flow of 1.8 million acre-feet per year. However, this discharge is extremely variable, there is a 30:1 ratio between the highest (1983, 4 million acre-feet) and lowest (1977, 135 thousand acre-feet) discharge years on record ("Tuolumne River," 2021). Several large dams were constructed to manage this variability, primarily for water supply, hydropower, and irrigation purposes. In the upper Tuolumne River, the Lake Eleanor, and Cherry Creek Dams discharge in to Hetch Hetchy Dam, which collectively provide the San Francisco Bay Area with both power and water. In the lower Tuolumne River near the town of Modesto, Don Pedro and La Grange Dams originally built in 1923 and enlarged in 1971, produce hydropower and play a leading role in preserving the state's water supply by holding salinity in the San Joaquin delta near the site of the State Water Project to acceptable standards (Water Resources Department, Contra Costa Water District, 2010). New Don Pedro Dam (the name given after its modification in 1971) is by far the largest of these Dams with a capacity of over 2 million acre-feet. It is the 10th tallest dam in the United States. Despite its size, New Don Pedro Dam, which is primarily used for irrigation and power generation, has one of the smallest flood pools in the central valley system with only 340 thousand acre-feet of dedicated flood storage (Virk & Hinky, 2021).

Data Analysis

The climate scenarios are simulated in a rainfall-runoff model (HEC-HMS). This model includes 28 subbasins, each containing calibrated time-to-concentration, two-bucket soil moisture accounting, temperature lapse rate, and degree-day snowmelt models. Evapotranspiration is modeled across the watershed using Priestly-Taylor methods that effectively simplify the Penman-Monteith equations, but retains an explicit energy balance that is important in climate change studies ("Chapter 2 - FAO Penman-Monteith equation," 2021; Lofgren et al., 2011). Inflows to up- (Cherry Creek, Eleanor, and Hetch Hetchy) and down-stream (Don Pedro and La Grange) dams are aggregated on 3-hour intervals. The system operations closely follow those published in the reservoirs' water control manuals and Federal Energy

Regulatory Commission (FERC) documentation. Hedging rules are empirically linked to the San Joaquin River Index (SJRI). In this study they were approximated using a set of Tuolumne River Watershed state variables like precipitation and snowpack that over the calibration and validation periods showed a strong correlation with the SJRI. The results focus primarily on flood and drought performance metrics at or downstream of New Don Pedro Dam near the watershed outlet. These metrics and the threshold values presented in the results were collected during workshops with the Turlock Irrigation District, which operates the reservoir, and the California Department of Water Resources, which plays a leading role in the operation of the larger San Joaquin River Watershed system and California State Water Project.

Results

This results section analyzes the climate scenarios' impact on flood and drought metrics, such as the end of water year storage at New Don Pedro Dam, irrigated water deliveries from Don Pedro Dam and the frequency and severity of flood events, as measured by the peak 3-hour stream flow exceeding 9,000 cubic feet per second at a flood gauge near the town of Modesto – downstream of Don Pedro Dam. These flood and water supply outcomes are modulated by snowpack conditions, which are controlled by climate variables like temperature and precipitation. Therefore, a discussion of April 1st snow water equivalent (SWE), which is particularly relevant to water supply outcomes, is also included.

Snow Water Equivalent

Summer water demands drive New Don Pedro water supply releases, and these releases are met by storing spring and summertime snowmelt. Consequently, the April 1st SWE, which approximates the annual maximum SWE, is treated by San Joaquin water managers as a harbinger of the season's water supply reliability. Figure 1 (in the figures section below) shows the shift in the distribution of snowpack conditions under 23 thermodynamically driven scenarios. Reductions in snowpack under climate change are dominated by the level of warming. Through warming alone, median April 1 SWE is reduced by 65 percent, under 2 degrees of warming, and 74 percent, under 4 degrees of warming. Under 2 degrees of warming, the median baseline April 1 SWE of 876 thousand acre-feet (TAF) is exceed in fewer than 20 percent of years. Under 4 degrees of warming, the baseline median SWE is exceeded on average once every 350 years.

Shifts and annual average precipitation, of ± 3 percent per degree of warming, and increases the intensity of extreme precipitation, of 7 percent per degree of warming (associated with thermodynamically driven increases in water vapor), are introduced as thermodynamic perturbations. Their marginal impact on snowpack were evaluated independent of shifts in temperature, to better understand the role they play

in flood and drought vulnerabilities. However, they were found to produce no meaningful change in the snowpack distributions. As a thermodynamic perturbation, the snowpack distribution shows minimal sensitivity to increases in intensity of extreme precipitation, with thermodynamically driven Clausius-Clapeyron perturbations producing, at most, a 4 percent reduction in the median SWE, when compared to an equivalent scenario with warming alone.

Thermodynamically motivated shifts in the annual average precipitation have a more meaningful impact on the median April 1 SWE. Increases in annual precipitation of 3 percent per degree of warming partially stem losses produced by warming only scenarios by 5, 8, and 14 percent (over the comparable scenarios with 2, 3, and 4 degrees of warming alone). Reductions in annual average precipitation decrease the median April 1st snowpack at nearly double this rate with additional 8, 16 and 23 percent reductions over comparison scenarios containing 2, 3, and 4 degrees of warming alone. In sum, under 4 degrees of warming, with a thermodynamically driven 12 percent reduction and average annual precipitation the baseline median April 1st SWE is reduced by 80 percent to 178 TAF. In fact, under this scenario there is less than 100 TAF of snow storage on April 1st in approximately 1/3 of all years.

Figure 2 (in the figures section below) shows the change in the maximum annual SWE under the same 23 scenarios. These results mirror the April 1 results since maximum annual snowpack typically occurs between April and May 1. However, under scenarios of increased warming the date of maximum snowpack is slightly reduced, further underscoring the storyline of increased wintertime rain and melt.

Water Supply

Figure 3 (in the figures section below) demonstrates a clear shift in the mode of the end of water year (i.e., Oct 1) water storage at new Don Pedro Dam from approximately 1750 TAF toward 1150 TAF, a 35 percent reduction in end of year supplies. This shift is associated with increased rationing and lower irrigation canal deliveries, displayed in Figure 4 (in the figures section below). Overall, median end of water year storage is expected to decline by roughly 10 percent per degree of warming, from 1500 TAF under baseline condition to 1350 and 1220 TAF under 2 and 4 degrees of warming, respectively. Shifts in annual mean precipitation and the intensity of extreme precipitation events do not substantially alter these results, increasing or decreasing the water supplies under the warming alone scenarios by less than 5 percent.

Flood Risk

Figure 5 (in the figures section below), shows the impact of climate perturbations on a synthetic version of the 1997 flood of record. This includes: (a) a 7 percent phase shift from snow to rain during the

event, and (b) a 52 percent reduction in snowpack over the course of the event. Cumulatively, these impacts associated with warming lead to a 24 percent increase in inflows into Don Pedro during the event. The 14 percent increase in the intensity of most extreme periods of precipitation during the event, result in a 14 percent increase in Don Pedro inflows. The combined impact, of warming plus increases in the intensity of extreme precipitation is an over 40 percent increase in Don Pedro inflows during the event. Figure 6 (in the figures section below) shows the total number of flood events, defined by flows exceeding 10,000 cubic feet per second (cfs) at the Modesto flood gauge under 23 climate scenarios. Warming and mean shifts in precipitation lead to a dramatic increase in the number of flood events. For instance, 4 degrees of warming alone is associated with a 4-fold increase in the number of flood events. Mean shifts in annual precipitation have little impact on the number of flood events in the absence of warming. However, as a set of thermodynamic scenarios, shifts in mean annual precipitation substantially exacerbate or blunt the impact of warming. For instance, under 4 degrees of warming a 12 percent increase in mean annual precipitation results in a more than 2-fold increase in the number of flood event, compared to the scenario with 4 degrees of warming alone. However, a 12 percent reduction in mean annual precipitation results in an 80 percent reduction in the same 4-fold increase that is experienced under 4 degrees of warming alone.

Conclusions

To manage water resources systems under climate change, planners require future scenarios describing the range of plausible threats facing their systems. To-date, impact assessments have followed two paths. Top-down assessments generate a limited set of convincing future scenarios that are unable to describe the range of threats facing water resource systems. Bottom-up analyses assert an ability to sample the range of plausible future vulnerabilities though exploratory analysis, but in practice it is rarely possible to assess the plausibility of these scenarios. This paper demonstrates a middle ground in which vulnerability-based assessments are driven by exploratory scenarios grounded in process-informed insight. This approach advances our ability to describe the impact of climate change on water resources. It also represents a logical step in the path toward the dynamic control of water resources systems under climate change (Herman et al., 2020). Under this dynamic planning paradigm, sources of thermodynamic and dynamic climate change credibly linked to indicator variables at a variety of spatial and temporal scales are used to trigger adaptive actions. This paper makes progress in the direction of this more durable solution to the climate change problem by demonstrating the link between local water resource vulnerability and plausible ranges of regional-to-global scale climate change features.

References

Allan, R. P., Barlow, M., Byrne, M. P., Cherchi, A., Douville, H., Fowler, H. J., et al. (2020). Advances in understanding large-scale responses of the water cycle to climate change. *Annals of the New York Academy of Sciences*, *1472*(1), 49–75. https://doi.org/10.1111/nyas.14337

Bankes, S. (1993). Exploratory Modeling for Policy Analysis. *Operations Research*, *41*(3), 435–449. https://doi.org/10.1287/opre.41.3.435

Barton, Y., Giannakaki, P., von Waldow, H., Chevalier, C., Pfahl, S., & Martius, O. (2016). Clustering of Regional-Scale Extreme Precipitation Events in Southern Switzerland. *Monthly Weather Review*, *144*(1), 347–369. https://doi.org/10.1175/MWR-D-15-0205.1

Blackport, R., & Screen, J. A. (2020). Weakened evidence for mid-latitude impacts of Arctic warming. *Nature Climate Change*, *10*(12), 1065–1066. https://doi.org/10.1038/s41558-020-00954-y

Brown, C., Ghile, Y., Laverty, M., & Li, K. (2012). Decision scaling: Linking bottom-up vulnerability analysis with climate projections in the water sector. *Water Resources Research*, *48*(9). https://doi.org/10.1029/2011WR011212

Brown, J. R., Lengaigne, M., Lintner, B. R., Widlansky, M. J., van der Wiel, K., Dutheil, C., et al. (2020). South Pacific Convergence Zone dynamics, variability and impacts in a changing climate. *Nature Reviews Earth & Environment*, *1*(10), 530–543. https://doi.org/10.1038/s43017-020-0078-2

Cai, W., Cowan, T., & Thatcher, M. (2012). Rainfall reductions over Southern Hemisphere semi-arid regions: the role of subtropical dry zone expansion. *Scientific Reports*, *2*(1), 702. https://doi.org/10.1038/srep00702

California Data Exchange Center. (2021). Retrieved June 1, 2021, from https://cdec.water.ca.gov/

Chapter 2 - FAO Penman-Monteith equation. (2021). Retrieved June 2, 2021, from http://www.fao.org/3/X0490E/x0490e06.htm

Cosgrove, B. A., Lohmann, D., Mitchell, K. E., Houser, P. R., Wood, E. F., Schaake, J. C., et al. (2003). Real-time and retrospective forcing in the North American Land Data Assimilation System (NLDAS) project. *Journal of Geophysical Research: Atmospheres*, *108*(D22). https://doi.org/10.1029/2002JD003118

Don Pedro Project Relicensing FERC No.2299 - Home. (2021). Retrieved June 1, 2021, from http://www.donpedro-relicensing.com/default.htm

Fowler, H. J., Blenkinsop, S., & Tebaldi, C. (2007). Linking climate change modelling to impacts studies: recent advances in downscaling techniques for hydrological modelling. *International Journal of Climatology*, *27*(12), 1547–1578. https://doi.org/10.1002/joc.1556

Fredriksen, H.-B., Berner, J., Subramanian, A. C., & Capotondi, A. (2020). How Does El Niño–Southern Oscillation Change Under Global Warming—A First Look at CMIP6. *Geophysical Research Letters*, *47*(22), e2020GL090640. https://doi.org/10.1029/2020GL090640

Grotch, S. L., & MacCracken, M. C. (1991). The Use of General Circulation Models to Predict Regional Climatic Change. *Journal of Climate*, *4*(3), 286–303. https://doi.org/10.1175/1520-0442(1991)004<0286:TUOGCM>2.0.CO;2

HEC-WAT. (2021). Retrieved June 2, 2021, from https://www.hec.usace.army.mil/software/hec-wat/

Herman, J. D., Zeff, H. B., Lamontagne, J. R., Reed, P. M., & Characklis, G. W. (2016). Synthetic Drought Scenario Generation to Support Bottom-Up Water Supply Vulnerability Assessments. *Journal of Water Resources Planning and Management*, *142*(11), 04016050. https://doi.org/10.1061/(ASCE)WR.1943-5452.0000701

Herman, J. D., Quinn, J. D., Steinschneider, S., Giuliani, M., & Fletcher, S. (2020). Climate Adaptation as a Control Problem: Review and Perspectives on Dynamic Water Resources Planning Under Uncertainty. *Water Resources Research*, *56*(2), e24389. https://doi.org/10.1029/2019WR025502

Kalnay, E., Kanamitsu, M., Kistler, R., Collins, W., Deaven, D., Gandin, L., et al. (1996). The NCEP/NCAR 40-Year Reanalysis Project. *Bulletin of the American Meteorological Society*, *77*(3), 437–471.

Karger, D. N., Schmatz, D. R., Dettling, G., & Zimmermann, N. E. (2020). High-resolution monthly precipitation and temperature time series from 2006 to 2100. *Scientific Data*, *7*(1), 248. https://doi.org/10.1038/s41597-020-00587-y

Kornhuber, K., Osprey, S., Coumou, D., Petri, S., Petoukhov, V., Rahmstorf, S., & Gray, L. (2019). Extreme weather events in early summer 2018 connected by a recurrent hemispheric wave-7 pattern. *Environmental Research Letters*, *14*(5), 054002. https://doi.org/10.1088/1748-9326/ab13bf

Lempert, R. J. (2019). Robust Decision Making (RDM). In V. A. W. J. Marchau, W. E. Walker, P. J. T. M. Bloemen, & S. W. Popper (Eds.), *Decision Making under Deep Uncertainty: From Theory to Practice* (pp. 23–51). Cham: Springer International Publishing. https://doi.org/10.1007/978-3-030-05252-2_2

Lenderink, G., Barbero, R., Loriaux, J. M., & Fowler, H. J. (2017). Super-Clausius–Clapeyron Scaling of Extreme Hourly Convective Precipitation and Its Relation to Large-Scale Atmospheric Conditions. *Journal of Climate*, *30*(15), 6037–6052. https://doi.org/10.1175/JCLI-D-16-0808.1

Livneh, B., Rosenberg, E. A., Lin, C., Nijssen, B., Mishra, V., Andreadis, K. M., et al. (2013). A Long-Term Hydrologically Based Dataset of Land Surface Fluxes and States for the Conterminous United States: Update and Extensions. *Journal of Climate*, *26*(23), 9384–9392. https://doi.org/10.1175/JCLI-D-12-00508.1

Lofgren, B. M., Hunter, T. S., & Wilbarger, J. (2011). Effects of using air temperature as a proxy for potential evapotranspiration in climate change scenarios of Great Lakes basin hydrology. *Journal of Great Lakes Research*, *37*(4), 744–752. https://doi.org/10.1016/j.jglr.2011.09.006

Martinkova, M., & Kysely, J. (2020). Overview of Observed Clausius-Clapeyron Scaling of Extreme Precipitation in Midlatitudes. *Atmosphere*, *11*(8), 786. https://doi.org/10.3390/atmos11080786

McCabe, G. J., & Dettinger, M. D. (1999). Decadal variations in the strength of ENSO teleconnections with precipitation in the western United States. *International Journal of Climatology*, *19*(13), 1399–1410. https://doi.org/10.1002/(SICI)1097-0088(19991115)19:13<1399::AID-JOC457>3.0.CO;2-A

Mendoza, G. F., Unesco, International Center for Integrated Water Resources Management, & International Hydrological Programme. (2018). *Climate risk informed decision analysis (CRIDA): collaborative water resources planning for an uncertain future*.

Pfahl, S., O'Gorman, P. A., & Fischer, E. M. (2017). Understanding the regional pattern of projected future changes in extreme precipitation. *Nature Climate Change*, *7*(6), 423–427. https://doi.org/10.1038/nclimate3287

Phillips, N. A. (1956). The general circulation of the atmosphere: A numerical experiment. *Quarterly Journal of the Royal Meteorological Society*, *82*(352), 123–164. https://doi.org/10.1002/qj.49708235202

Quinn, J. D., Reed, P. M., Giuliani, M., Castelletti, A., Oyler, J. W., & Nicholas, R. E. (2018). Exploring How Changing Monsoonal Dynamics and Human Pressures Challenge Multireservoir Management for Flood Protection, Hydropower Production, and Agricultural Water Supply. *Water Resources Research*, *54*(7), 4638–4662. https://doi.org/10.1029/2018WR022743

Ray, P. A., & Brown, C. M. (2015). Confronting Climate Uncertainty in Water Resources Planning and Project Design, 149.

Redmond, K. T., & Koch, R. W. (1991). Surface Climate and Streamflow Variability in the Western United States and Their Relationship to Large-Scale Circulation Indices. *Water Resources Research*, *27*(9), 2381–2399. https://doi.org/10.1029/91WR00690

Revelle, R., Broecker, W., Craig, H., Keeling, C. D., & Smagorinsky, J. (1965). *Restoring the Quality of Our Environment, Appendix Y4*. Washington, D.C.: Report of the Environmental Pollution Panel, President's Science Advisory Committee. Retrieved from https://ozonedepletiontheory.info/Papers/Revelle1965AtmosphericCarbonDioxide.pdf

Robertson, A. W., & Ghil, M. (1999). Large-Scale Weather Regimes and Local Climate over the Western United States. *Journal of Climate*, *12*(6), 1796–1813. https://doi.org/10.1175/1520-0442(1999)012<1796:LSWRAL>2.0.CO;2

Schlef, K. E., Moradkhani, H., & Lall, U. (2019). Atmospheric Circulation Patterns Associated with Extreme United States Floods Identified via Machine Learning. *Scientific Reports*, *9*(1), 7171. https://doi.org/10.1038/s41598-019-43496-w

Seager, R., Naik, N., & Vecchi, G. A. (2010). Thermodynamic and Dynamic Mechanisms for Large-Scale Changes in the Hydrological Cycle in Response to Global Warming. *Journal of Climate*, *23*(17), 4651–4668. https://doi.org/10.1175/2010JCLI3655.1

Steinschneider, S., & Brown, C. (2013). A semiparametric multivariate, multisite weather generator with low-frequency variability for use in climate risk assessments. *Water Resources Research*, *49*(11), 7205–7220. https://doi.org/10.1002/wrcr.20528

Steinschneider, S., Ray, P., Rahat, S. H., & Kucharski, J. (2019). A Weather-Regime-Based Stochastic Weather Generator for Climate Vulnerability Assessments of Water Systems in the Western United States. *Water Resources Research*, *55*(8), 6923–6945. https://doi.org/10.1029/2018WR024446

Swain, D. L. (2015). A tale of two California droughts: Lessons amidst record warmth and dryness in a region of complex physical and human geography. *Geophysical Research Letters*, *42*(22), 9999–10,003. https://doi.org/10.1002/2015GL066628

Teutschbein, C., & Seibert, J. (2012). Bias correction of regional climate model simulations for hydrological climate-change impact studies: Review and evaluation of different methods. *Journal of Hydrology*, *456–457*, 12–29. https://doi.org/10.1016/j.jhydrol.2012.05.052

Trenberth, K. E., Cheng, L., Jacobs, P., Zhang, Y., & Fasullo, J. (2018). Hurricane Harvey Links to Ocean Heat Content and Climate Change Adaptation. *Earth's Future*, *6*(5), 730–744. https://doi.org/10.1029/2018EF000825

Tuolumne River. (2021, January 20). In *Wikipedia*. Retrieved from https://en.wikipedia.org/w/index.php?title=Tuolumne_River&oldid=1001667389

Ullrich, P. A., Xu, Z., Rhoades, A. M., Dettinger, M. D., Mount, J. F., Jones, A. D., & Vahmani, P. (2018). California's Drought of the Future: A Midcentury Recreation of the Exceptional Conditions of 2012–2017. *Earth's Future*, *6*(11), 1568–1587. https://doi.org/10.1029/2018EF001007

Vigaud, N., Robertson, A. W., & Tippett, M. K. (2018). Predictability of Recurrent Weather Regimes over North America during Winter from Submonthly Reforecasts. *Monthly Weather Review*, *146*(8), 2559–2577. https://doi.org/10.1175/MWR-D-18-0058.1

Virk, S., & Hinky, J. (2021). Don Pedro Dam. Retrieved March 16, 2021, from https://watershed.ucdavis.edu/shed/lund/dams/Don%20Pedro/donpedro.htm

Water Resources Department, Contra Costa Water District. (2010). *Historical Fresh Water and Salinity Conditions in the Western Sacramento-San Joaquin Delta and Suisun Bay: A Summary of Historical Reviews, Reports, Analyses and Measurements* (Technical Memorandum No. WR 10-001). Concord, California. Retrieved from https://cawaterlibrary.net/wp-content/uploads/2017/10/swrcb_ccwd2010.pdf

Wehrli, K., Guillod, B. P., Hauser, M., Leclair, M., & Seneviratne, S. I. (2018). Assessing the Dynamic Versus Thermodynamic Origin of Climate Model Biases. *Geophysical Research Letters*, *45*(16), 8471–8479. https://doi.org/10.1029/2018GL079220

Wilby, R., Charles, S., Zorita, E., Timbal, B., Whetton, P., & Mearns, L. (2004). Guidelines for Use of Climate Scenarios Developed from Statistical Downscaling Methods, 27.

Wilby, R. L., & Dessai, S. (2010). Robust adaptation to climate change. *Weather*, *65*(7), 180–185. https://doi.org/10.1002/wea.543

Yun, K.-S., Lee, J.-Y., Timmermann, A., Stein, K., Stuecker, M. F., Fyfe, J. C., & Chung, E.-S. (2021). Increasing ENSO–rainfall variability due to changes in future tropical temperature–rainfall relationship. *Communications Earth & Environment*, *2*(1), 1–7. https://doi.org/10.1038/s43247-021-00108-8

Zscheischler, J., Westra, S., van den Hurk, B. J. J. M., Seneviratne, S. I., Ward, P. J., Pitman, A., et al. (2018). Future climate risk from compound events. *Nature Climate Change*, *8*(6), 469–477. https://doi.org/10.1038/s41558-018-0156-3

Zscheischler, J., Martius, O., Westra, S., Bevacqua, E., Raymond, C., Horton, R. M., et al. (2020). A typology of compound weather and climate events. *Nature Reviews Earth & Environment*, *1*(7), 333–347. https://doi.org/10.1038/s43017-020-0060-z

Figures

Figure 1. April 1 Snowpack

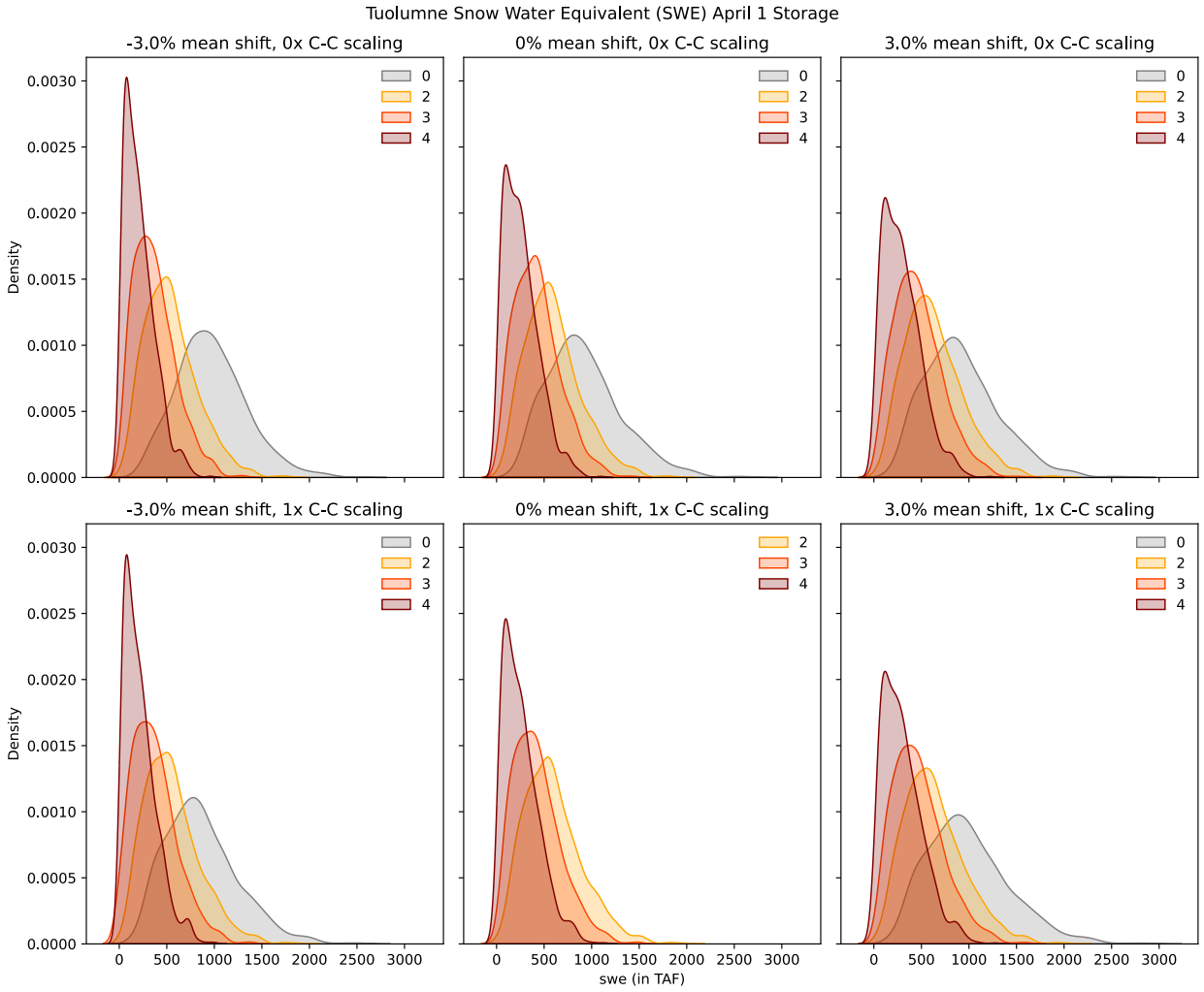

Figure 2. Annual Maximum Snowpack

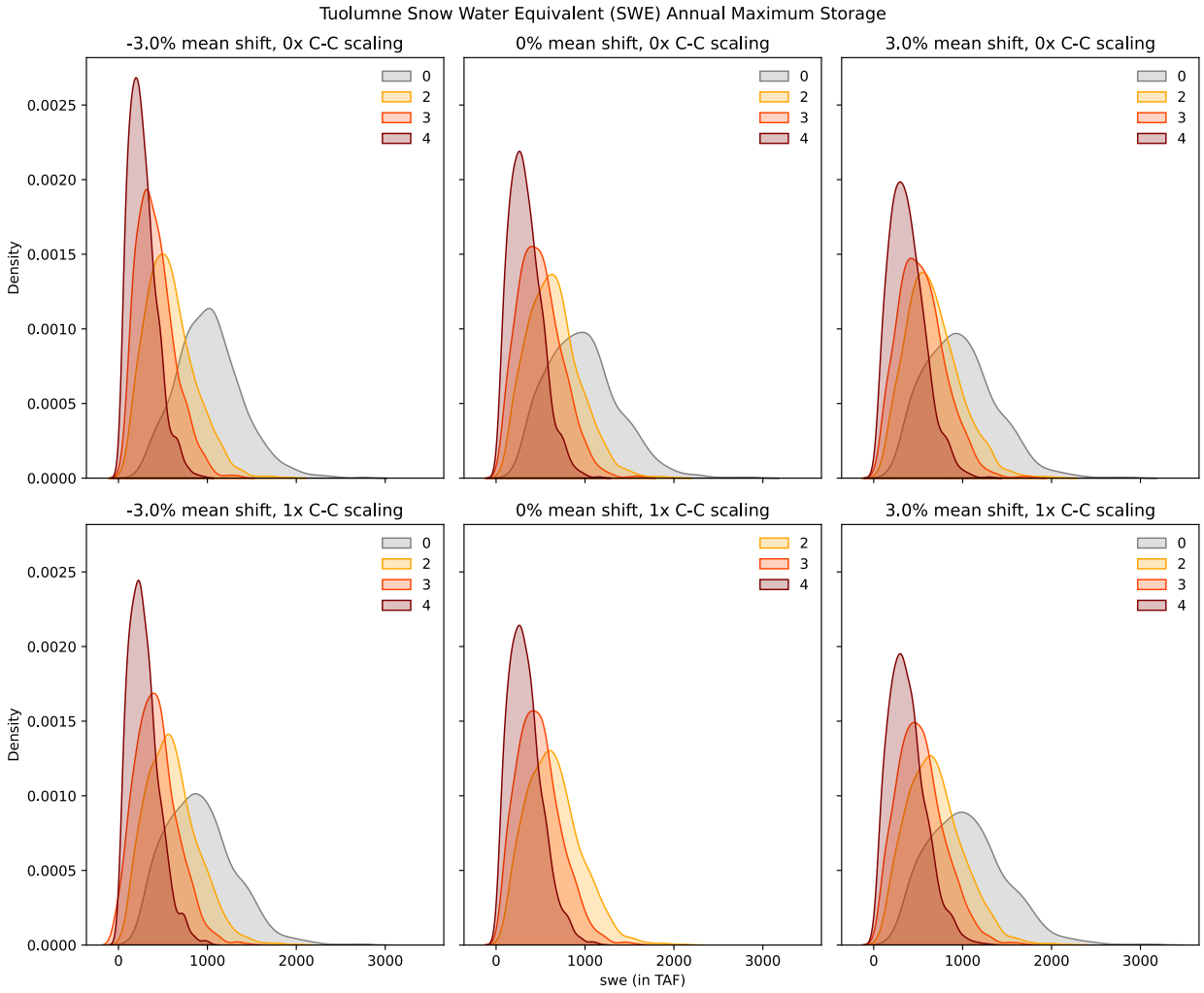

Figure 3. October 1 Storage

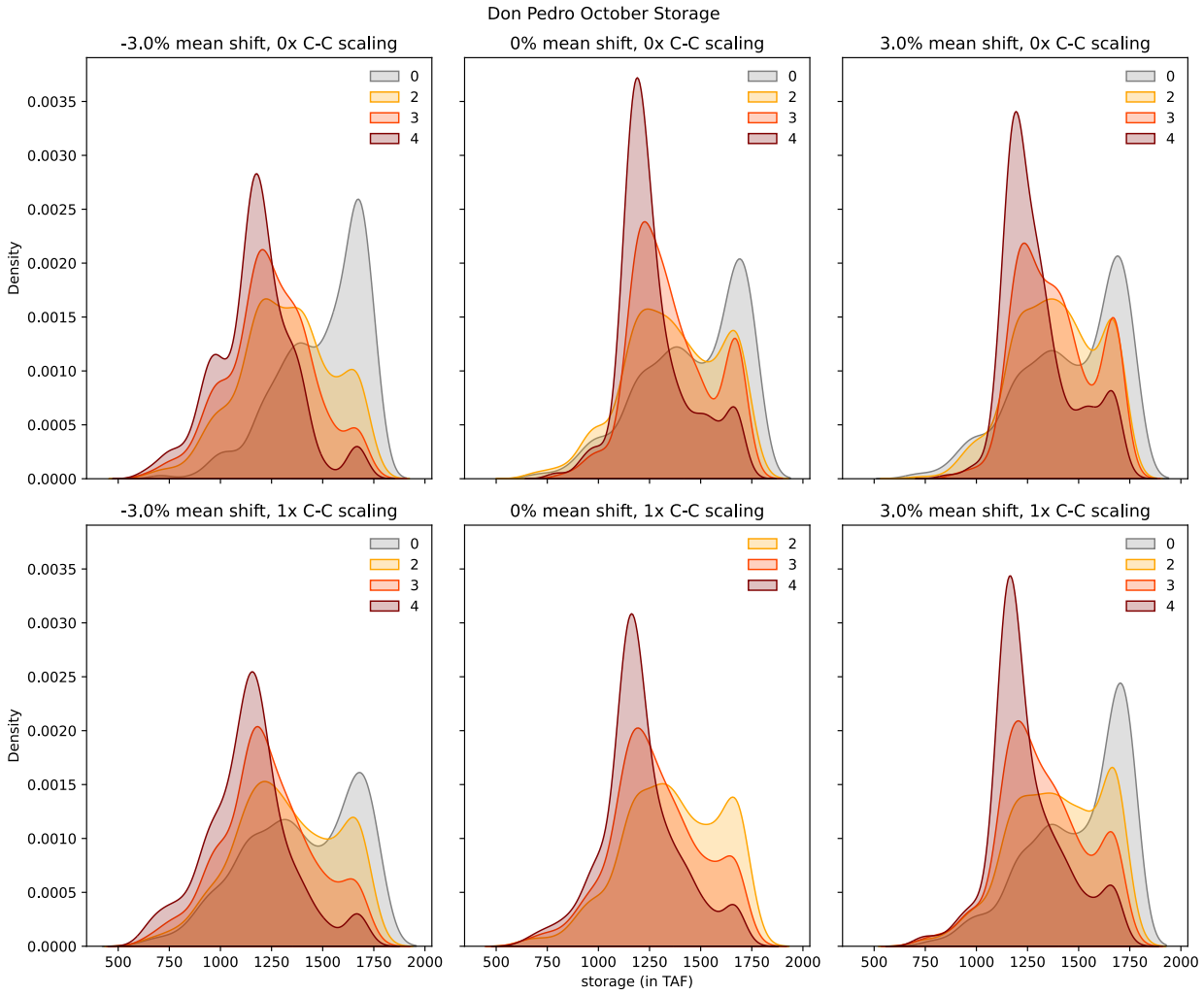

Figure 4. Don Pedro Irrigation Canal Deliveries

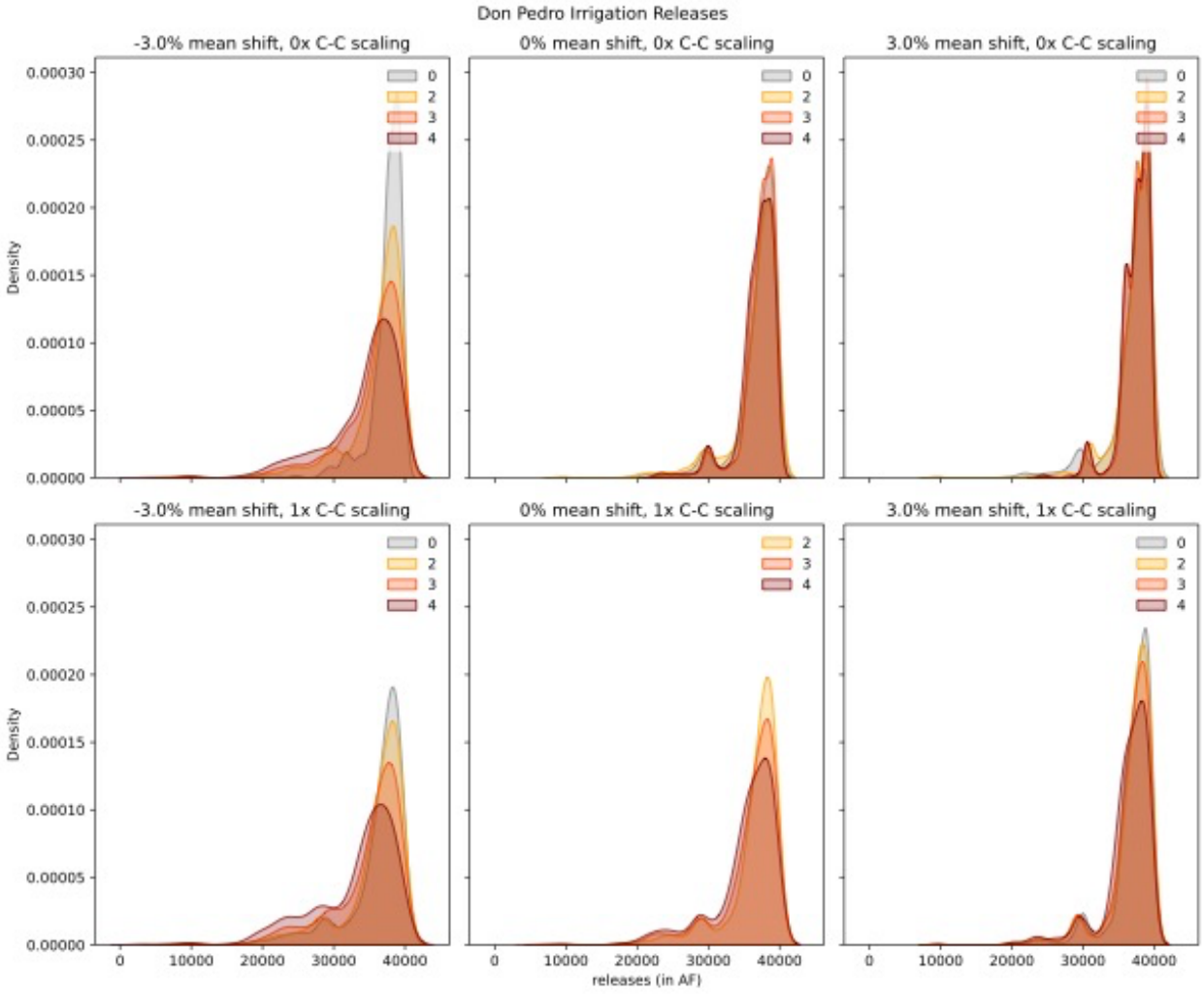

Figure 5. Impact of Climate Perturbation on Synthetic 1997 Event

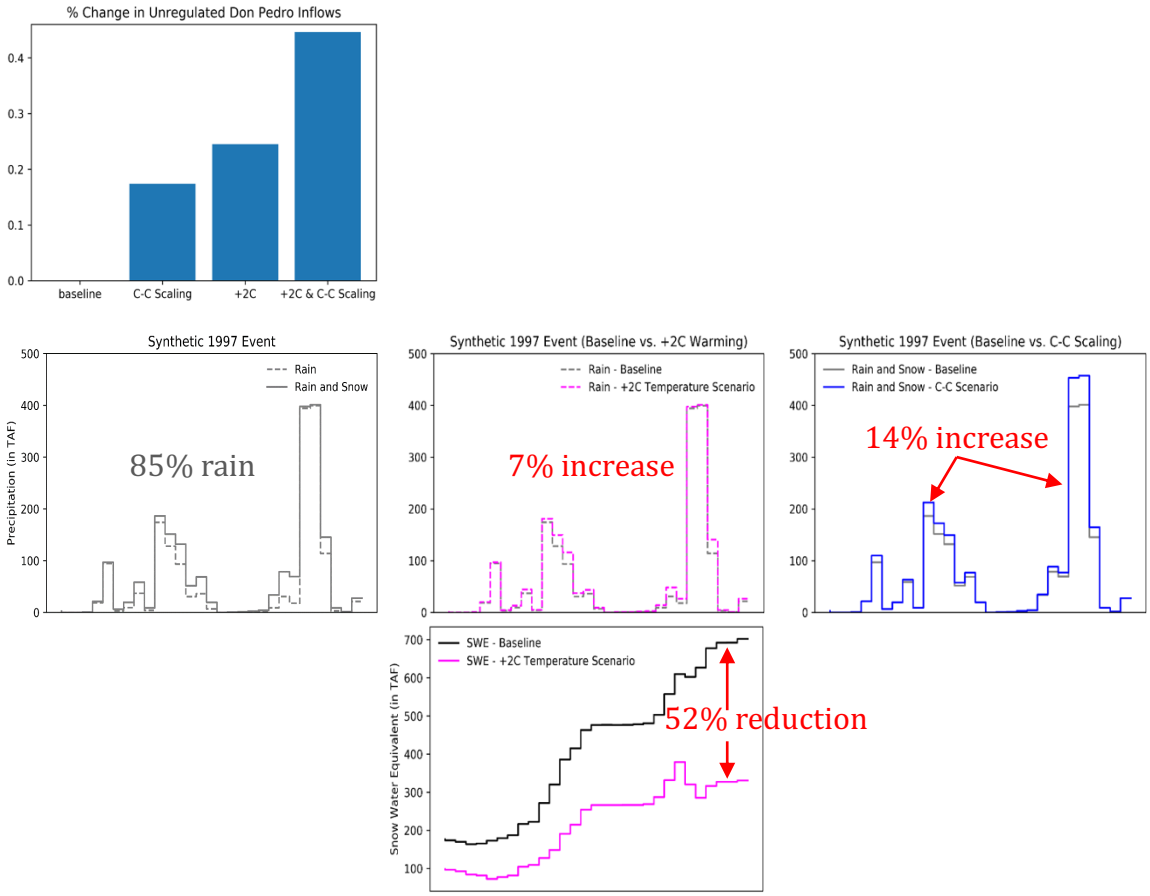

Figure 6. Flood Events (Flow > 10,000 Cubic Feet per Second at Modesto Flood Gauge)